



## Short communication

## Large-scale preparation of barium sulphate nanoparticles in a high-throughput tube-in-tube microchannel reactor

Qi-An Wang<sup>a</sup>, Jie-Xin Wang<sup>a</sup>, Min Li<sup>a</sup>, Lei Shao<sup>b,\*</sup>, Jian-Feng Chen<sup>a,\*\*</sup>, Lin Gu<sup>c</sup>, Yong-Tao An<sup>c</sup><sup>a</sup> Key Lab for Nanomaterials, Ministry of Education, Beijing University of Chemical Technology, Beijing 100029, PR China<sup>b</sup> Research Center of the Ministry of Education for High Gravity Engineering and Technology, Beijing University of Chemical Technology, Beijing 100029, PR China<sup>c</sup> Advanced Technology & Materials Co., Ltd., Beijing 100081, PR China

## ARTICLE INFO

## Article history:

Received 24 October 2008

Received in revised form 22 January 2009

Accepted 13 February 2009

## Keywords:

Tube-in-tube microchannel reactor

Large-scale preparation

Barium sulphate

High throughput

Micromixing

## ABSTRACT

One method for increasing productivity of a microreactor is presented without demanding numbering-up processes by using a newly proposed microporous tube-in-tube microchannel reactor (MTMCR) with a high throughput of 9 L/min. Barium sulphate nanoparticles with an average size of 37 nm and a narrow size distribution were successfully produced in MTMCR. The size of barium sulphate particles was strongly dependent on the flow rate of the reactants in the microchannel and high flow rate was beneficial for producing small particles. Furthermore, it was possible to control the average particle size in the range from 30 to 150 nm by changing the reactant concentrations and the micropore size on the surface of the inner tube. The average particle size decreased by increasing the total flow rate and reactant concentrations or decreasing the micropore size. The dispersed-phase flow rate and mixing distance exhibited little effects on the particle size. The proposed microreactor concept was confirmed to be valid and promising for the industrial production of nanoparticles.

© 2009 Elsevier B.V. All rights reserved.

## 1. Introduction

The rapid development of microtechnology in recent years has led to a considerable variety of microdevices. Because of their highly efficient micromixing performance and short transport time, microdevices, in particular microreactors, are commercially available with numerous designs and materials nowadays [1]. In general, microreactors are continuous flow-type reactors and are defined as miniaturized reaction systems, which are fabricated by use of methods of microtechnology and precision engineering [2]. Their characteristic dimensions of internal structures are less than 1 mm in size [3,4]. The main feature of microreactors is the high surface-area-to-volume ratio, which gives prospect of better heat and mass transfer rates compared to conventional reactors and allows reactions under severe conditions to be performed with higher yield or selectivity.

Nanoparticles are attracting interest because of their distinct physical and chemical properties. The preparation of nanoparticles is a very significant and challenging work. Among all the methods of producing nanomaterials, the liquid–liquid chemosynthesis is the

most efficient and widely used one that traditionally proceeds in batch reactors [5]. However, it is difficult to control the reaction precisely in a batch reactor because of the poor mixing and mass transfer performance. It is expected that microreactors will overcome this problem and produce nanoparticles with narrow size distribution, because microreactors provide a reaction volume or a microchannel that is more homogeneous with respect to concentration, temperature, and mass transfer, leading to a better control of reaction or the precipitation step that governs the particle size and its distribution, i.e., nucleation and growth [6]. Thus, many organizations have recently joined the research of using microchannel reactors to prepare nanoparticles such as semiconductors [7–9], metals [10,11], colloids [12], zeolite [13], and organic compounds [14], etc. These works demonstrated that microchannel reactors were suitable for the continuous preparation of nanoparticles and exhibited great advantages in controlling reaction conditions and particle properties.

However, the production capacities of most reported microreactors, usually at  $\mu\text{L}$  or  $\text{mL}/\text{min}$  scale, are much smaller than those of conventional reactors owing to their specific structures [15–17], which is hard to meet the demand of industrial production for high throughput. Currently, there are two pathways in increasing the productivity of reaction products, or in scale-up process: (a) the construction of reaction modules, so-called numbering-up, and (b) the improvement of a reactor itself. This paper concerns the latter pathway. A new structured microdevice, designated micro-

\* Corresponding author. Tel.: +86 10 64421706; fax: +86 10 64423474.

\*\* Corresponding author. Tel.: +86 10 64446466; fax: +86 10 64434784.

E-mail addresses: shaol@mail.buct.edu.cn (L. Shao), chenjf@mail.buct.edu.cn (J.-F. Chen).

porous tube-in-tube microchannel reactor (MTMCR), is proposed. In MTMCR, two coaxial tubes form annular microchannel, and micropores on one section of the inner tube are employed as the dispersion media. The liquid going through the annular micropore belt from inside the inner tube is split into many radial microstreams, followed by high-speed impinging cross-currently with the laminar flow in the annular chamber between inner and outer tubes, thereby exhibiting the combined effects of many T-type microchannels with good micromixing and large throughput.

Barium sulphate is a kind of important inorganic chemical product and widely used as packing materials and additives in painting, coating and plastics. Nanosized barium sulphate has more scientific advantages of size reduction. Liquid–liquid precipitation reaction is the main preparation method of  $\text{BaSO}_4$  nanoparticles. Furthermore, the precipitation of barium sulphate is also a commonly used experimental system for evaluating the micromixing performance of reactors [17–21]. The process can reveal the effect of micromixing on the crystal size, size distribution and morphology. Therefore, we carried out the preparation of  $\text{BaSO}_4$  nanoparticles in MTMCR to test the micromixing performance and evaluate the possibility for the large-scale production of uniform  $\text{BaSO}_4$  nanoparticles. The throughput of the novel microreactor can reach up to 9 L/min or even larger (typical microreactors: 4–100 mL/min [8–11,15,17]), but its mixing performance is still excellent.

## 2. Experimental section

### 2.1. Materials and setup

Analytical reagent (AR) grade sodium sulphate and barium chloride were purchased from Beijing Reagent Factory of China. Deionized water was obtained from a water purification system (RO-DI plus, Hitech, PRC).

Schematic diagram of the experimental setup (a) and MTMCR photographs (b) are illustrated in Fig. 1. There are two main parts in the microreactor: the inner tube (J) and outer tube (K). A lot of micropores (G) are distributed around the wall at one end of the inner tube (micropore zone: porosity of 46%; length of 1 cm).

The microporous section of the microreactor is composed of several layers of metal meshes. Each mesh was weaved with stainless steel wires of a certain diameter. These meshes were assembled layer by layer with the mesh of larger wire diameter on the surface as a protection layer, followed by pre-calcination, rolling and calcination at 1280 °C for 3 h to obtain the microporous materials. The microporous materials were then rounded and welded to form the annular microporous section of the reactor. The pore size of the microporous materials was determined by a bubbling method and the porosity was determined by a comparison of the density of the microporous materials with that of steel.

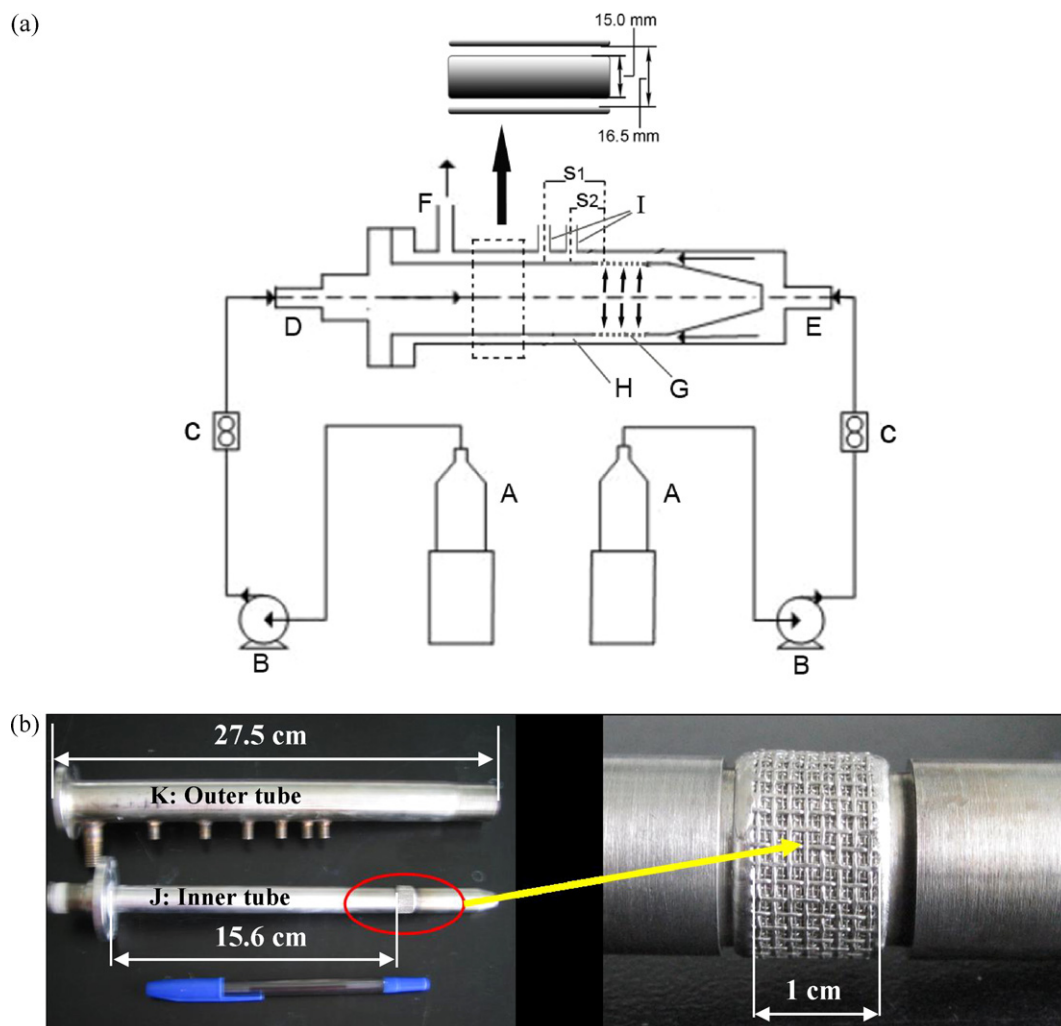


**Fig. 1.** (a) Schematic diagram of experimental set-up and the structure of the reactor: A, tank; B, pump; C, flowmeter; D, inlet of inner tube; E, inlet of outer tube; F, outlet; G, micropores; H, microchannel; I, sample points. (b) Photographs of microporous tube-in-tube microreactor: (left) inner tube (J) and outer tube (K); (right) microporous section.

In this microreactor, the dispersed solution (phase) is forced to flow from the inner tube through the micropores into the annular chamber (H) to mix with the continuous phase from the outer tube. The inner tubes with pore sizes of 5  $\mu\text{m}$ , 10  $\mu\text{m}$ , 20  $\mu\text{m}$  and 40  $\mu\text{m}$  were employed in this study. The width of the mixing chamber (the distance between the inner and outer tubes) is 750  $\mu\text{m}$ . Several sampling points (I) are designed along the axial position of the outer tube to explore the effect of mixing distance on the particle size.

### 2.2. Reactive precipitation process

$\text{Na}_2\text{SO}_4$  and  $\text{BaCl}_2 \cdot 2\text{H}_2\text{O}$  were separately dissolved in deionized water and then filtered through the membranes with 0.45  $\mu\text{m}$  pore size to remove the particulate impurities prior to use.  $\text{BaCl}_2$  solution (dispersed phase) and  $\text{Na}_2\text{SO}_4$  solution (continuous phase) were pumped into the inner and outer tubes (D, E) respectively with two magnetic pumps (B) at room temperature (25  $^\circ\text{C}$ ). After passing through the micropores of the inner tube,  $\text{BaCl}_2$  solution was dispersed into microstreams and reacted with  $\text{Na}_2\text{SO}_4$  solution in the annular chamber to form  $\text{BaSO}_4$  precipitates, which were collected at the outlet (F) by a beaker containing supersaturated  $\text{BaSO}_4$  solution to stop further growth and aggregation of  $\text{BaSO}_4$  particles. The as-obtained  $\text{BaSO}_4$  suspension was then sampled and dispersed in deionized water for SEM observation.

### 2.3. Characterization

The morphology of  $\text{BaSO}_4$  particles was characterized by field emission scanning electron microscope (FE-SEM, Hitachi S-4700), and  $\text{BaSO}_4$  particle size and size distribution were determined using IBAS I/II Image Analyzer System (Germany).

## 3. Results and discussion

### 3.1. Morphology and particle size distribution

It is expected that varying the flow rate of the reactants will have a considerable influence on the size distribution of the particles. Fig. 2 shows typical FE-SEM images of  $\text{BaSO}_4$  nanoparticles prepared by mixing 0.35 mol/L  $\text{BaCl}_2$  solution with 0.1 mol/L  $\text{Na}_2\text{SO}_4$  solution at three flow rates. When the flow rates of  $\text{BaCl}_2$  and  $\text{Na}_2\text{SO}_4$  solutions were 1.71 and 6 L/min or 2 and 7 L/min, respectively, the particle sizes were mainly distributed at the range of 30–60 nm, which are much smaller than the size of those (range: 1–10  $\mu\text{m}$ ) precipitated in Taylor-Couette reactor or other classic stirred tank reactors [19–23]. Particle size is affected by the micromixing performance and better micromixing results in smaller particles [23]. It can be concluded that MTMCR has better micromixing performance compared with other reactors.

The particle size distributions of the as-prepared  $\text{BaSO}_4$  nanoparticles are given in Fig. 3. It can be found that the average particle size decreased with the increase of the flow rate. The possible reason is that an increase of the flow rate results in both the increase of the supersaturation (responsible for smaller average size) and improvement of the micromixing (responsible for uniform size distribution), both of which favor the precipitation of nanosized particles with narrower size distribution.

### 3.2. Influence of the distance between microporous section and sampling points

The influence of the distance between the microporous section and the sampling points, which is defined as mixing distance  $S$ , on the average size of  $\text{BaSO}_4$  nanoparticles is presented in Fig. 4. The average particle size  $d_p$ , obtained from measuring each particle size

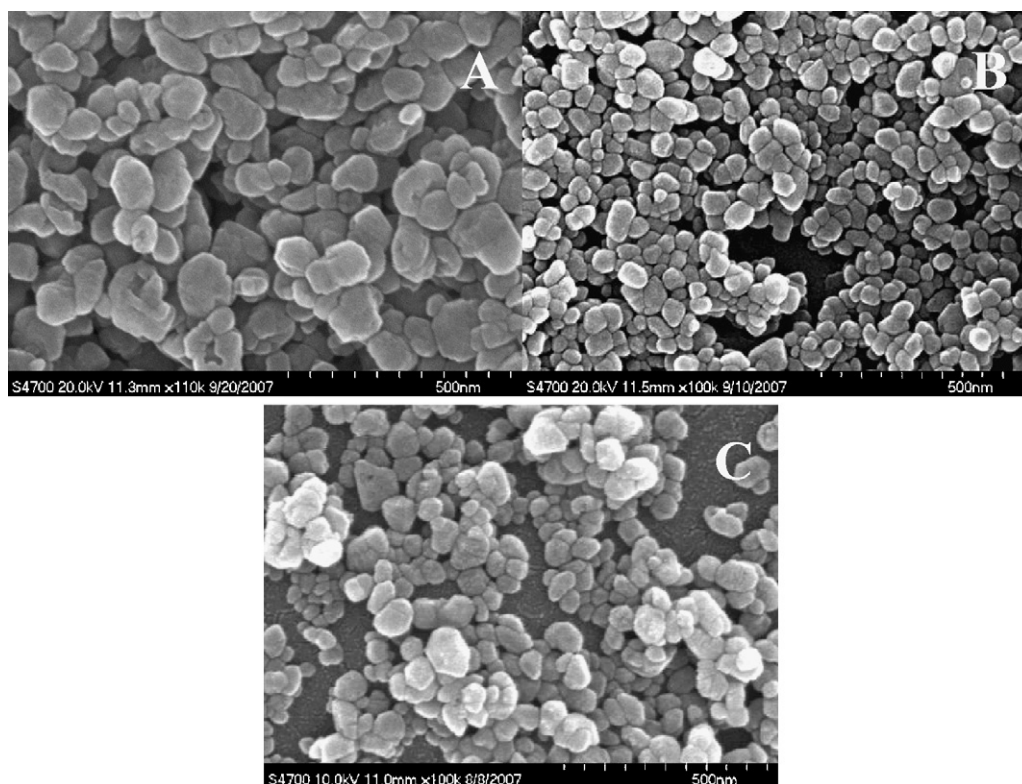


**Fig. 2.** FE-SEM images of  $\text{BaSO}_4$  nanoparticles prepared at different flow rates of  $\text{BaCl}_2$  and  $\text{Na}_2\text{SO}_4$  solutions: (A) 0.57 and 2 L/min; (B) 1.71 and 6 L/min; (C) 2 and 7 L/min ( $\text{BaCl}_2$ : 0.35 mol/L,  $\text{Na}_2\text{SO}_4$ : 0.1 mol/L, 40  $\mu\text{m}$  pore size).

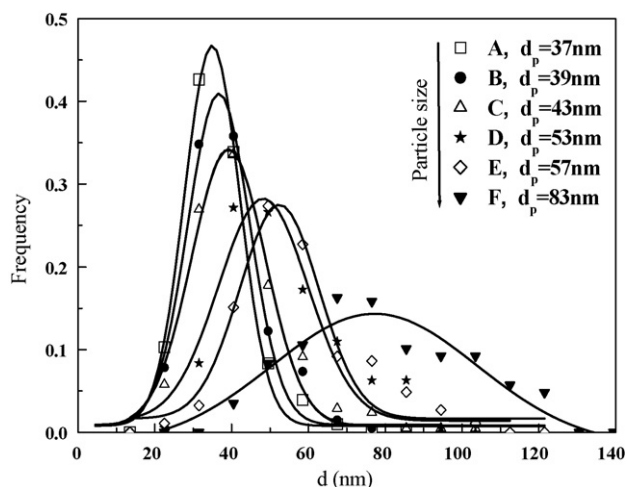


**Fig. 3.** Size distribution of BaSO<sub>4</sub> particles prepared at different flow rates of BaCl<sub>2</sub> and Na<sub>2</sub>SO<sub>4</sub> solutions: (A) 2 and 7 L/min; (B) 1.71 and 6 L/min; (C) 1.43 and 5 L/min; (D) 0.57 and 2 L/min; (E) 0.39 and 1.35 L/min; (F) 0.29 and 1 L/min.

in FE-SEM images, is defined as:

$$d_p = \frac{\sum d_i}{N}$$

where  $d_i$  is the size of each particle and  $N$  is the number of the particles.

Although  $S$  varied from 4 to 160 mm, no significant effect on the average size of particles was observed, implying that the excellent micromixing performance in this microreactor results in the fast completion of the precipitation reaction. From the practical point of view, this is convenient because it allows setting up the entire experiment flexibly according to different needs [1]. Moreover, both the cost of the microreactor and the energy consumption can be reduced via regulating  $S$  in an industrial setting.

### 3.3. Influence of reactant flow rate

The effects of the total flow rate  $F$  of the two phases and the dispersed phase flow rate  $F_d$  on the average particle size of BaSO<sub>4</sub> are given in Figs. 5 and 6, respectively. The corresponding Reynolds ( $Re$ ) numbers are also indicated in these two figures. It can be deduced from  $Re$  numbers that the flow is violently turbulent in the reaction chamber, exhibiting excellent mixing effect. With the increase of the total flow rate,  $Re$  number increases and the turbulence and

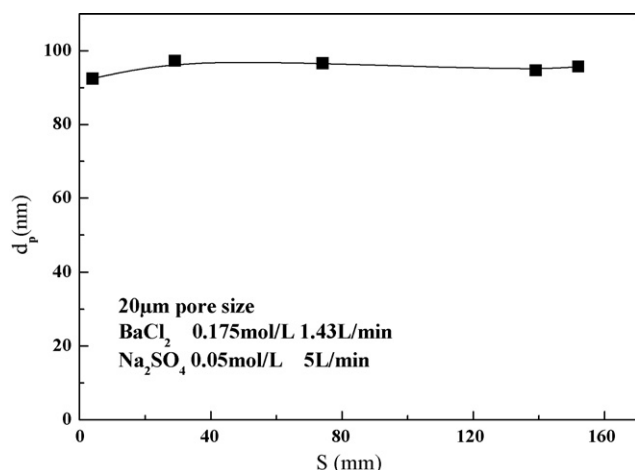


**Fig. 4.** Influence of the mixing distance  $S$  on the average particle size  $d_p$ .

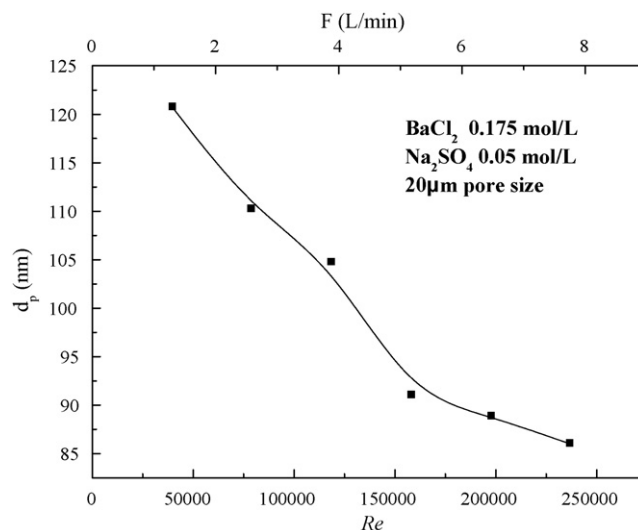


**Fig. 5.** Influence of the total flow rate and the corresponding Reynolds ( $Re$ ) number on  $d_p$ .

mixing effects are enhanced, which are favorable for convection and interdiffusion of reactants, resulting in an even nucleation and particle growth environment and leading to a small particle size and uniform particle size distribution. On the contrary, low mixing effectiveness of reactants leads to uneven distribution of supersaturation profiles under the reaction environment, thereby leading to a non-uniform distribution of the driving force for the nucleation and growth processes and giving rise to wide crystal size distributions [24].

Fig. 6 shows that no evident change in the particles size is observed at a fixed micropore size of 20  $\mu\text{m}$  when only varying the flow rate of BaCl<sub>2</sub>, i.e., the dispersed phase, indicating that the micropores exert much more significant influence on micromixing than the flow rate of the dispersed phase.

### 3.4. Influence of reactant concentration

Fig. 7 exhibits the influence of the reactant concentration on the formation of BaSO<sub>4</sub> nanoparticles. The average particle size decreased quickly by increasing the concentrations of BaCl<sub>2</sub> and

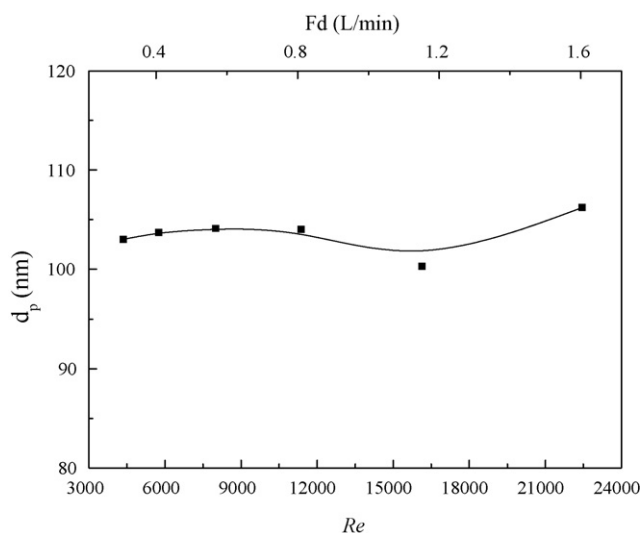


**Fig. 6.** Influence of the dispersed phase flow rate and the corresponding Reynolds ( $Re$ ) number on  $d_p$  (pore size: 20  $\mu\text{m}$ ).

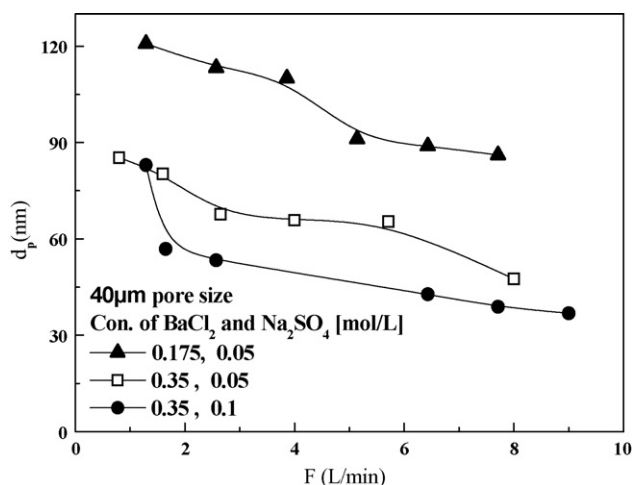


Fig. 7. Influence of the reactant concentration on  $d_p$ .

$\text{Na}_2\text{SO}_4$  solutions proportionally. Generally, supersaturation is the thermodynamic driving force for nucleation and growth in the precipitation reaction. The increases of  $\text{Na}_2\text{SO}_4$  and  $\text{BaCl}_2$  concentrations resulted in a high supersaturation level, which made nucleation and crystal growth proceed very fast, leading to the generation of small particles [25]. Furthermore, it can be seen in Fig. 7 that at fixed  $\text{Na}_2\text{SO}_4$  or  $\text{BaCl}_2$  concentration, the average particle size decreased evidently with the increase of  $\text{BaCl}_2$  concentration from 0.175 to 0.35 mol/L or  $\text{Na}_2\text{SO}_4$  concentration from 0.05 to 0.1 mol/L. Obviously,  $\text{Na}_2\text{SO}_4$  concentration plays the same role as  $\text{BaCl}_2$  concentration in particle size. This is well consistent with the traditional theories about the kinetic equations of nucleation and growth, in which the weight coefficients of the concentrations are equivalent

### 3.5. Influence of micropore size

Fig. 8 displays the effect of the micropore size on the average sizes of  $\text{BaSO}_4$  nanoparticles. When the total flow rate ranged from 2.57 to 3.86 L/min, the average particle size was substantially influenced by the micropore size. The particle size decreased with a decrease of the micropore size. There was only a little difference of the obtained particle size between 40 and 20  $\mu\text{m}$  micropore size. However, as the pore size was reduced to 10 or 5  $\mu\text{m}$ , the average

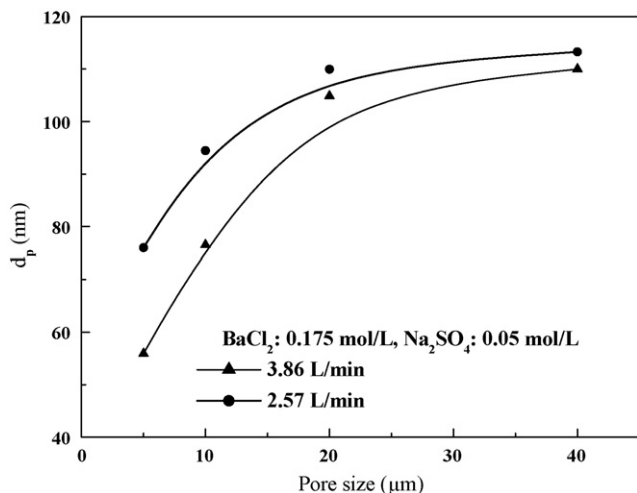


Fig. 8. Influence of the micropore size on  $d_p$ .

particle size sharply decreased owing to the obvious enhancement of the mixing performance. This is because the size of dispersed phase is mainly determined by the micropore size. The micromixing between  $\text{BaCl}_2$  and  $\text{Na}_2\text{SO}_4$  solutions was greatly improved by decreasing the micropore size, thereby resulting in small  $\text{BaSO}_4$  particle size and narrow size distribution.

## 4. Conclusions

A new microreactor was presented for nanoparticle production in this paper. A simple and robust method has been successfully developed to produce size-controllable  $\text{BaSO}_4$  nanoparticles at high throughput of 9 L/min by utilizing the microporous tube-in-tube microchannel reactor (MTMCR). The effects of the flow rate, reactant concentration, micropore size, as well as mixing distance on the average particle size were investigated. The average particle size decreases due to improved micromixing performance or higher supersaturation by increasing the total flow rate and phase concentrations or decreasing the micropore size, a major contributing factor to micromixing performance. The dispersed-phase flow rate and mixing distance have little effects on the particle size. MTMCR demonstrates unique advantages over conventional microreactors in nanoparticle production due to the high-throughput feature.

In the preparation of nanoparticles by MTMCR, a smaller micropore size is required to generate smaller particles. However, the throughput of the reactor will be affected unfavorably by the increase of the flow resistance resulting from a smaller micropore size. It is deduced that the product quality and the throughput of the reactor may be adjusted by changing the porosity of the microporous section and the distance between the outer tube and the inner tube, which also exert significant influence on the production of nanoparticles.

## Acknowledgements

This work was financially supported by National “863” Program of China (No. 2007AA030207), National Natural Science Foundation of China (Nos. 20806004 and 20821004) and National “973” Program of China (No. 2009CB219903).

## References

- [1] S. Panić, S. Loebbecke, T. Tuercke, J. Antes, D. Bošković, Experimental approaches to a better understanding of mixing performance of microfluidic devices, *Chem. Eng. J.* 101 (2004) 409–419.
- [2] H. Löwe, W. Ehrfeld, State-of-the-art in microreaction technology: concepts, manufacturing and applications, *Electrochim. Acta.* 44 (1999) 3679–3689.
- [3] K.F. Jensen, Microreaction engineering—is small better? *Chem. Eng. Sci.* 56 (2001) 293–303.
- [4] K. Jahnisch, V. Hessel, H. Löwe, M. Baerns, Chemistry in microstructured reactors, *Angew. Chem. Int. Ed.* 43 (2004) 406–446.
- [5] B.L. Cushing, V.L. Kolesnichenko, C.J. O'Connor, Recent advances in the liquid-phase syntheses of inorganic nanoparticles, *Chem. Rev.* 104 (2004) 3893–3946.
- [6] J. deMello, A. deMello, Microscale reactors: nanoscale products, *Lab. Chip* 4 (2004) 11N–15N.
- [7] B.K.H. Yen, N.E. Stott, K.F. Jensen, M.G. Bawendi, A continuous-flow microcapillary reactor for the preparation of a size series of CdSe nanocrystals, *Adv. Mater.* 15 (2003) 1858–1862.
- [8] E.M. Chan, R.A. Mathies, A.P. Alivisatos, Size-controlled growth of CdSe nanocrystals in microfluidic reactors, *Nano Lett.* 3 (2003) 199–201.
- [9] J.B. Edel, R. Fortt, J.C. deMello, A.J. deMello, Microfluidic routes to the controlled production of nanoparticles, *Chem. Commun.* 2 (2002) 1136–1137.
- [10] X.Z. Lin, A.D. Terepka, H. Yang, Synthesis of silver nanoparticles in a continuous flow tubular microreactor, *Nano Lett.* 4 (2004) 2227–2232.
- [11] J. Wagner, T. Kirner, G. Mayer, J. Albert, J.M. Köhler, Generation of metal nanoparticles in a microchannel reactor, *Chem. Eng. J.* 101 (2004) 251–260.
- [12] S.A. Khan, A. I. Gunther, M.A. Schmidt, K.F. Jensen, Microfluidic synthesis of colloidal silica, *Langmuir* 20 (2004) 8604–8611.
- [13] J.X. Ju, C.F. Zeng, L.X. Zhang, N.P. Xu, Continuous synthesis of zeolite NaA in a microchannel reactor, *Chem. Eng. J.* 116 (2006) 115–121.
- [14] T. Kawaguchi, H. Miyata, K. Ataka, K. Mae, J. Yoshida, Room-temperature swern oxidations by using a microscale flow system, *Angew. Chem. Int. Ed.* 44 (2005) 2413–2416.

- [15] Y. Ying, G.W. Chen, Y.C. Zhao, S.L. Li, Q. Yuan, A high throughput methodology for continuous preparation of monodispersed nanocrystals in microfluidic reactors, *Chem. Eng. J.* 135 (2008) 209–215.
- [16] H. Okamoto, T. Ushijima, O. Kitoh, New methods for increasing productivity by using microreactors of planar pumping and alternating pumping types, *Chem. Eng. J.* 101 (2004) 57–63.
- [17] G.G. Chen, G.S. Luo, S.W. Li, J.H. Xu, J.D. Wang, Experimental approaches for understanding mixing performance of a minireactor, *AIChE. J.* 51 (2005) 2923–2929.
- [18] E.D. McCarthy, W.A.E. Dunk, K.V.K. Boodhoo, Application of an intensified narrow channel reactor to the aqueous phase precipitation of barium sulphate, *J. Colloid Interf. Sci.* 305 (2007) 72–87.
- [19] M. Aoun, E. Plasari, R. David, J. Villermaux, Are barium sulphate kinetics sufficiently known for testing precipitation reactor models? *Chem. Eng. Sci.* 51 (1996) 2449–2458.
- [20] A.A. Barresi, D. Marchisio, G. Baldi, On the role of micro- and mesomixing in a continuous Couette-type precipitator, *Chem. Eng. Sci.* 54 (1999) 2339–2349.
- [21] J. Baldyga, O. Wojciech, Barium sulphate precipitation in a pipe – an experimental study and CFD modeling, *Chem. Eng. Sci.* 56 (2001) 2435–2444.
- [22] R. Pohorecki, J. Baldyga, The use of a new model of micromixing for determination of crystal size in precipitation, *Chem. Eng. Sci.* 38 (1985) 79–83.
- [23] B. Judat, A. Racina, M. Kind, Macro- and micromixing in a Taylor-Couette reactor with axial flow and their influence on the precipitation of barium sulphate, *Chem. Eng. Technol.* 27 (2004) 287–292.
- [24] G. Trippa, R.J.J. Jachuck, Precipitation of calcium carbonate using narrow channel reactors, *Trans. IChemE A* 81 (2003) 766–772.
- [25] M. Kucher, D. Babic, M. Kind, Precipitation of barium sulphate: experimental investigation about the influence of supersaturation and free lattice ion ratio on particle formation, *Chem. Eng. Proc.* 4 (2006) 900–907.